



OPEN ACCESS

EDITED BY

Alexandre Marcowith, UMR5299 Laboratoire Univers et Particules de Montpellier (LUPM), France

REVIEWED BY Andrei Bykov, Ioffe Institute (RAS), Russia

*CORRESPONDENCE Emanuele Greco,

RECEIVED 02 October 2025 REVISED 24 October 2025 ACCEPTED 29 October 2025 PUBLISHED 11 November 2025

Greco E (2025) From shock to synchrotron: a mini-review on magnetic turbulence in supernova remnants Front. Astron. Space Sci. 12:1717808. doi: 10.3389/fspas.2025.1717808

COPYRIGHT

© 2025 Greco. This is an open-access article distributed under the terms of the Creative Commons Attribution License (CC BY). The use, distribution or reproduction in other forums is permitted, provided the original author(s) and the copyright owner(s) are credited and that the original publication in this journal is cited, in accordance with accepted academic practice. No use, distribution or reproduction is permitted which does not comply with these terms.

From shock to synchrotron: a mini-review on magnetic turbulence in supernova remnants

Emanuele Greco*

INAF-Osservatorio Astronomico di Palermo, Palermo, Italy

Magnetic turbulence plays a crucial role in confining charged particles near the shock front of Supernova Remnants, enabling them to reach energies up to hundreds of TeV through a process known as Diffusive Shock Acceleration (DSA). These high-energy electrons spiral along magnetic field lines, emitting Xray synchrotron radiation. The launch of the Imaging X-ray Polarimetry Explorer (IXPE) has opened a new window into the study of magnetic fields in SNRs through X-ray polarization measurements. For the first time, IXPE allows us to resolve the polarization degree (PD) and angle (PA) in the X-ray band across different areas of SNRs, offering direct insight into the geometry and coherence of magnetic fields on different scales. In this mini-review, I summarize the key observational results on SNRs obtained with IXPE over the past 4 years and discuss their implications for our understanding of magnetic turbulence in synchrotron-emitting regions. I also show how we can combine polarization parameters and standard X-ray spectral/imaging analysis to better constrain the structure and scale of magnetic turbulence immediately downstream of the shock and understand the particle acceleration occurring in SNRs.

KEYWORDS

supernova remnants, particle acceleration, synchrotron radiation, magnetic turbulence, X-ray polarization, X-rayobservations

1 Introduction

Shocks in supernova remnants (SNRs) are widely recognized as prime candidates for the acceleration of Galactic cosmic rays (CRs), primarily through the mechanism of Diffusive Shock Acceleration (DSA, Fermi, 1949; Blandford and Eichler, 1987). Within this framework, magnetic turbulence plays a crucial role as it confines charged particles near the shock front, enabling them to repeatedly cross it and gain energy up to PeV energies. The key parameter quantifying this degree of turbulence and the efficiency of particle acceleration is the Bohm factor $\eta = \lambda_{mfp}/r_g$, where λ_{mfp} is the mean free path of the charged particles and r_o their gyroradius. An equivalent expression relates η to the ratio between the ordered and turbulent components of the magnetic field B (provided that $B > \delta B$, i.e., in the linear regime): $\eta = \left\langle \frac{B}{\delta B} \right\rangle^2$ (see, e.g., Vink, 2020). For $\eta = 1$, in the so-called Bohm diffusion the scattering regime is the most efficient with the particle scattered once per gyro-orbit. The acceleration time scale t_{acc} for relativistic particles under DSA is (Malkov and O'C Drury, 2001; Parizot et al., 2006; Helder et al., 2012):

$$t_{acc} = \eta \frac{E}{3eB} V_s^{-2} \tag{1}$$

where E is the electron energy and V_s is the shock velocity. TeV electrons move along the magnetic field lines, emit X-ray synchrotron radiation cooling down in a characteristic timescale $t_{\rm loss}$

$$t_{\text{loss}} = 12 \left(\frac{B}{1 \text{ mG}}\right)^{-2} \left(\frac{E}{\text{TeV}}\right)^{-1} \text{yr}$$
 (2)

It is often useful to rewrite Equation 1 and Equation 2 as functions of the characteristic synchrotron energy ε_0 , which can be directly inferred from X-ray spectroscopic analysis (Equations 3, 4):

$$\begin{split} t_{acc} &\approx 2\,\eta \left(\frac{\varepsilon_0}{1\,\text{keV}}\right)^{0.5} \left(\frac{B}{1\,\text{mG}}\right)^{-3/2} \left(\frac{V_s}{3000\,\text{km/s}}\right)^{-2} \text{yr}; \\ t_{\text{loss}} &\approx 1.5 \left(\frac{\varepsilon_0}{1\,\text{keV}}\right)^{-0.5} \left(\frac{B}{1\,\text{mG}}\right)^{-3/2} \text{yr} \end{split} \tag{3}$$

When the acceleration time scale t_{acc} and the synchrotron loss time scale t_{loss} are comparable, we enter in the so-called loss-limited regime, i.e., the maximum energy of the electrons E_{max} is limited by their losses (Zirakashvili and Aharonian, 2007):

$$E_{\rm max} \approx 10 \, \eta^{-1/2} \left(\frac{B}{100 \, \mu \rm G} \right)^{-1/2} \left(\frac{V_{\rm s}}{3000 \, {\rm km/s}} \right) \approx 10 \left(\frac{\varepsilon_0}{1 \, {\rm keV}} \right)^{1/2} \left(\frac{B}{100 \, \mu \rm G} \right)^{-1/2} {\rm TeV}$$
 (4)

where I have used the relation (Zirakashvili and Aharonian, 2007; Tsuji et al., 2021; Sapienza et al., 2024) for the second part of the equation.

$$\varepsilon_0 = \frac{1.6}{\eta} \left(\frac{V_s}{4000 \,\text{km/s}} \right)^2 \text{keV} \tag{5}$$

From Equation 5, one can see that magnetic turbulence, expressed in the form of η , also affects the spectrum emitted from the charged particles. Equation 5 offers therefore a direct diagnostic on η from X-ray spectroscopic (to measure the cutoff photon energy) and imaging analysis (to measure the shock velocity through proper motion).

Observations with high-resolution X-ray instruments such as Chandra and XMM-Newton (see Helder et al., 2012 for a review) have revealed the presence of narrow synchrotron filaments immediately downstream of the shock. By measuring the thickness of these structures from the images, several studies (e.g., Vink and Laming, 2003) reported values $\gtrsim 100~\mu G$, much higher than the expected shock-compressed magnetic field of roughly $20~\mu G$, suggesting strong magnetic field amplification likely induced by CRs-driven instabilities (Bell, 2004). The strength of the amplified magnetic field depends on the density of the ambient medium ρ_0 and on the shock velocity V_s (Vink, 2006) $B^2 \propto \rho_0 V_s^3$, i.e., fast shocks better amplify the magnetic field (Blasi, 2013) but generate an higher level of magnetic turbulence.

Particle-in-cell (PIC) simulations by Caprioli and Spitkovsky (2014a), Caprioli and Spitkovsky (2014b) have shown that self-consistent acceleration of ions can excite magnetic turbulence both upstream and downstream of strong shocks, leading to $\delta B/B_0 \gtrsim 1$ and a turbulent spectrum characterized by broad-band fluctuations. In these simulations acceleration is most efficient (Bohm-like) for parallel magnetic fields and a radially oriented magnetic structure naturally originates downstream the shock through the Richtmyer-Meshkov instability (RMI, Richmyer, 1960; Meshkov, 1969). Given the small spatial scale in which such

simulations are performed, it's hard to immediately translate such structures to the astrophysical scales, but they certainly represent an important hint in understanding the origin of the radially-oriented magnetic field observed in the radio. Magneto-hydrodynamic (MHD) simulations (e.g., Inoue et al., 2013; Bykov et al., 2020) show that density fluctuations in the ambient medium can seed turbulence via RMI and Rayleigh-Taylor instabilities, which in turn amplify the magnetic field via a turbulent dynamo mechanism. These processes can produce magnetic structures with strengths up to $\sim 100~\mu G$ and reproduce the radial-to-tangential magnetic field morphologies observed in young remnants. It is therefore still matter of debate whether the upstream medium plays a role in shaping the downstream magnetic field and whether it could facilitate its amplification and the acceleration of particles.

1.1 Diagnostic on turbulence through X-ray polarization

The recent launch, in December 2021, of the Imaging X-ray Polarimetric Explorer (IXPE; Weisskopf et al., 2022) has opened a new channel to probe turbulence in SNRs: IXPE allows direct, spatially resolved measurements of the X-ray polarization degree (PD) and angle (PA), thus mapping the magnetic-field configuration across different SNRs regions. Since synchrotron radiation is intrinsically linearly polarized - up to ~70% depending on the spectral slope (Ginzburg and Syrovatskii, 1965) - any reduction reflects depolarizing effects such as those relative to magnetic-field amplification. Consequently, PD and PA measurements provide direct insight into the degree of magnetic-field order. Previously, only radio observations were suitable to measure the polarization in SNRs, showing radial fields for young SNRs (e.g., Cas A, Anderson et al., 1995; SN 1006; Reynoso et al., 2013) and tangential field for more evolved ones (e.g., G156.2 + 5.7, Xu et al., 2007; G57.2 + 0.8; Kothes et al., 2018). However, radio synchrotron radiation is originated by GeV electrons and not by the freshly accelerated TeV electrons responsible for the X-ray emission. Therefore, probing the conditions immediately behind the shock front, where the acceleration is still ongoing, can only be performed by looking at the X-ray polarization data.

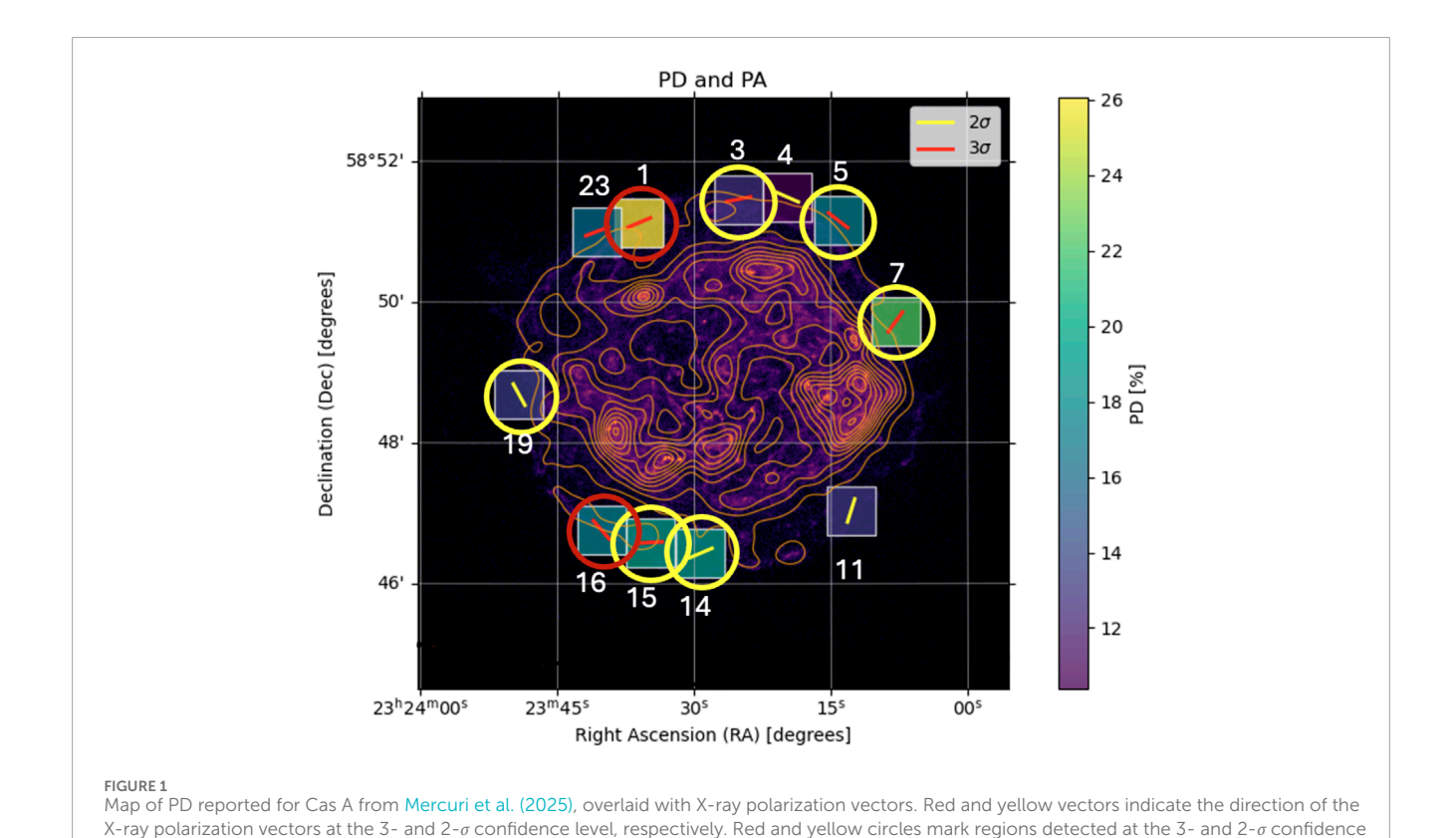
Table 1 highlights the main features of the sample of SNRs observed, completely or partially, by IXPE so far: Cas A, Tycho, the two limbs of SN1006, the north western region of RX J1713.7-3946 (Vela Jr) and a filament of Vela Jr.

1.1.1 Cas A

Cas A, a \sim 350 yr old core-collapse SNR, was the first science target observed by IXPE. Its forward shock velocity is of the order of 5000 km/s and shows a very low overall polarization level in the radio band of \sim 5% (e.g., Anderson et al., 1995) and a radial magnetic field (Rosenberg, 1970). Analysis performed by Vink et al. (2022) retrieved a value of 2%–5% in the PD for the whole shell and forward shock regions, lower than that observed in the radio, with a magnetic field radially oriented. Mercuri et al. (2025) re-analyzed the dataset adopting a different approach based on spectropolarimetric analysis: they fitted the IXPE spectra extracted from boxes across the whole shell by properly accounting for the thermal emission through the analysis of Chandra observations. They found PD values as high as

TABLE 1 Sample of SNRs observed by IXPE.

SNR	Age (yr)	B (μ G)	PD	V_s (km/s)	B orientation	References
Cas A (whole)	~350	~250	~2.5%	~5000	radial	Vink et al. (2022)
Cas A (regions)	~350	~250	10 -26%	~5000	radial	Mercuri et al. (2025)
Tycho's SNR	453	~200	~9%	~4000	radial	Ferrazzoli et al. (2023)
SN 1006 (NE)	1019	~80	~22%	~5000	radial	Zhou et al. (2023)
SN 1006 (SW)	1019	~80	20 -40%	~5000	radial	Zhou et al. (2025)
RX J1713 (NW)	~1500	~20	26%-30%	~4000	tangential	Ferrazzoli et al. (2024)
Vela Jr (NW)	~2000	~10	10%-20%	≥3000	tangential	Prokhorov et al. (2024)



level with the approach used by Vink et al. (2022), respectively. Superimposed in orange are the 3-6 keV Chandra contours.

26%, at more than the 3σ confidence level, highlighting that within relatively big and inhomogeneous regions it is possible to have an ordered magnetic field locally (Figure 1).

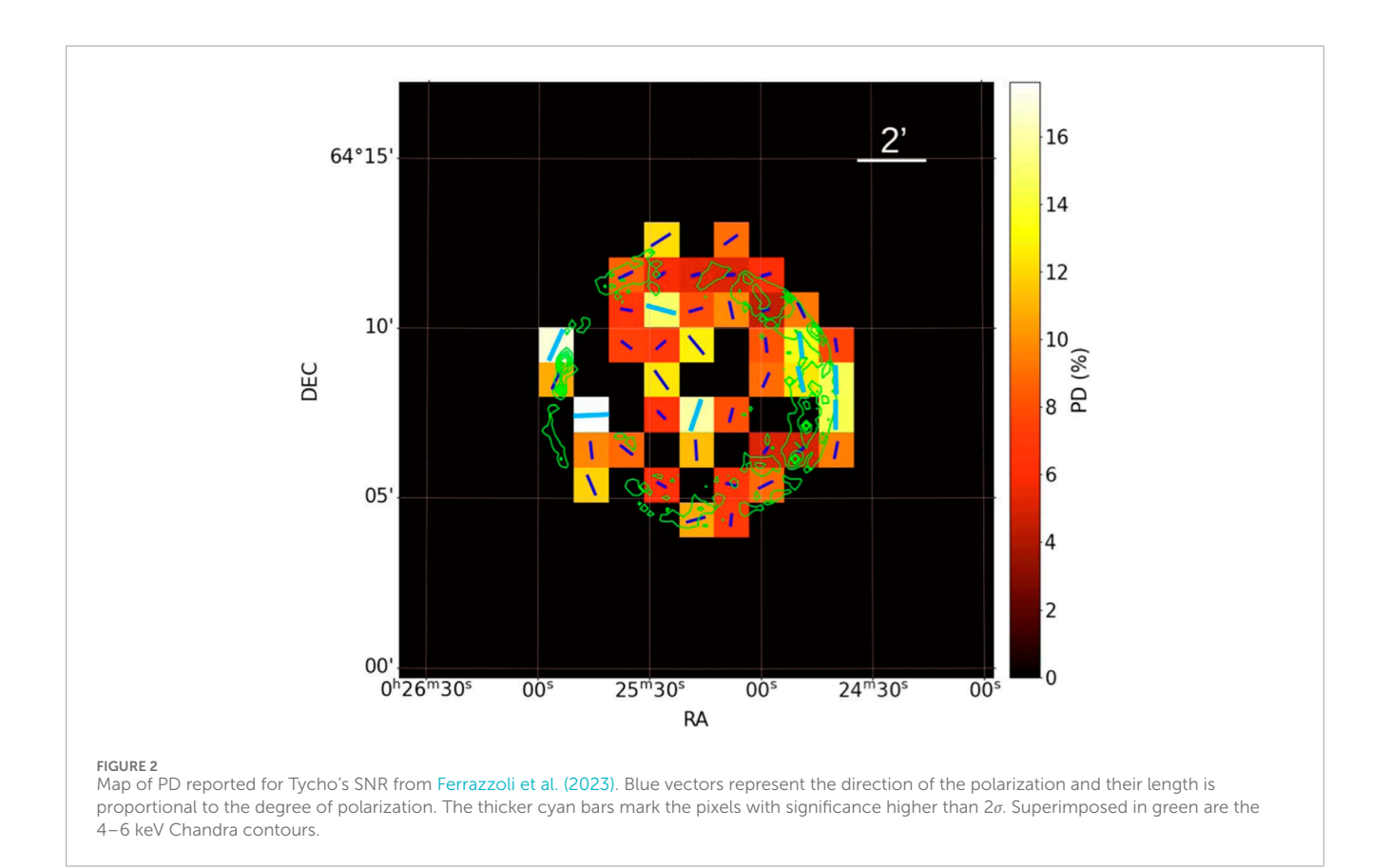
1.1.2 Tycho

The historical Tycho's SNR, exploded in 1572 is a Type Ia SNR, characterized by shock velocities of around 4,000 km/s (Williams et al., 2016). Significant radio polarization was found only in the outer rim at the \sim 7% level and the magnetic field was found to be radially oriented (Dickel et al., 1991). Tycho is characterised by thin X-ray synchrotron structures in the west, known as "stripes" and first identified by Eriksen et al. (2011) and characterised by

variations on scale of few years (Matsuda et al., 2020). The overall X-ray polarization was found to be 9% in the whole SNR and 12% if considering only the shell, where the synchrotron radiation is dominating (Ferrazzoli et al., 2023, see Figure 2). The stripes did not show a remarkably higher or lower PD with respect to the other regions.

1.1.3 SN 1006

The remnant of the historical SN 1006 is popular for being the first one for which X-ray synchrotron radiation was observed in its limbs (Koyama et al., 1995). IXPE observed both the NorthEastern (NE, Zhou et al., 2023) and SouthWestern (SW, Zhou et al., 2025)



limbs finding for both the limbs a radially-oriented magnetic field and an X-ray PD of ~22%, the highest reported for SNRs. However, the distribution of the PD is quite different between the two limbs (Figure 3). In the NE the PD is quite homogenous across the whole area, whereas in the SW the minimum value of PD is found in a region known to interact with an HI cloud (Miceli et al., 2014) and peaks up to ~40% where there is no interaction. This is suggestive of environment-dependent magnetic turbulence and magnetic field amplification.

1.1.4 RX J1713.7-3946

RX J1713.7-3946 (hereafter RX J1713) is a close (~1 kpc) and large SNR having a diameter of roughly 1°. Its X-ray emission is completely synchrotron-dominated, with the only exception for a detection of shocked ejecta in the inner area (Katsuda et al., 2015). At odds with the other SNRs discussed so far, IXPE observations of the NW area of RX J1713 indicated a tangential magnetic field and an overall polarization degree of roughly 12% (Ferrazzoli et al., 2024, left panel in Figure 4). This could be either due to the higher age of the SNR, in analogy with what observed for evolved SNRs in the radio band, or to the different environment in which the shock is expanding, characterized by dense molecular clouds.

1.1.5 Vela Jr

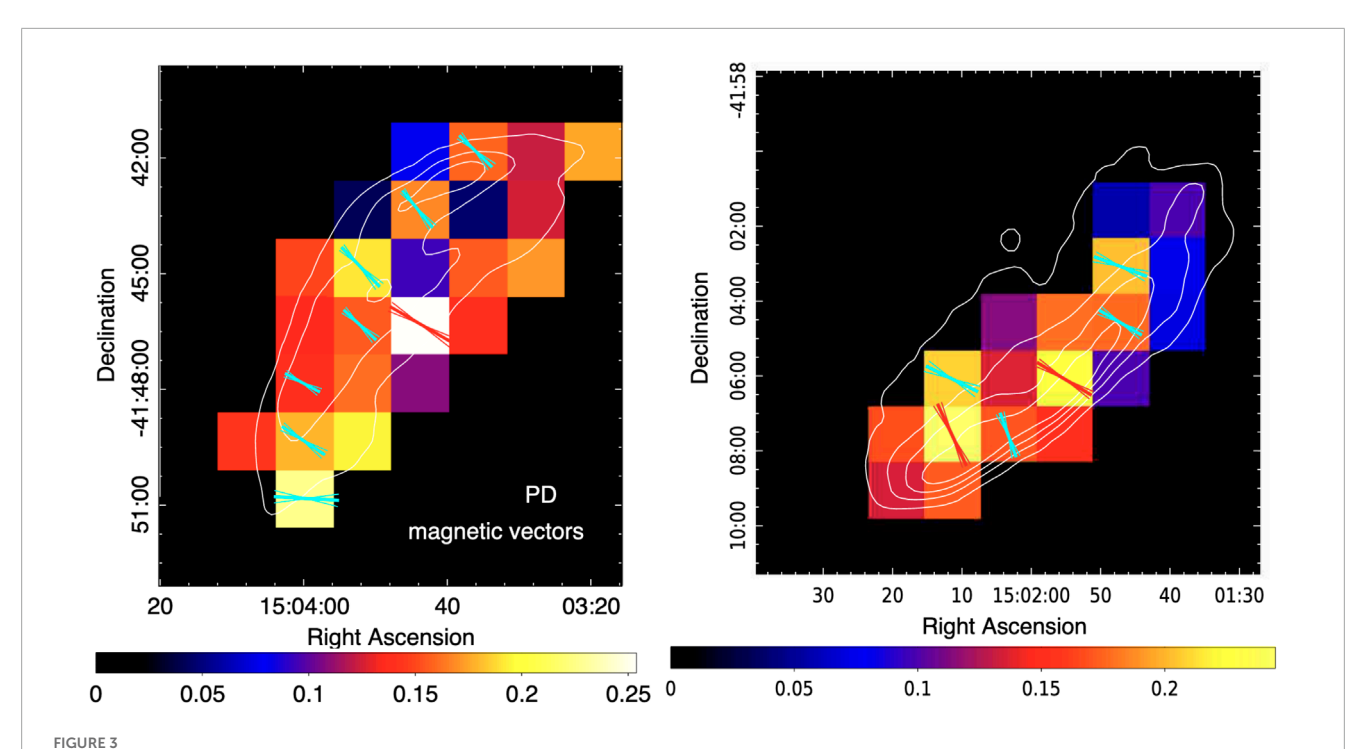
Vela Jr shares several features with RX J1713, being dominated by X-ray nonthermal emission, having an angular size of roughly 2° and being roughly 2000 years old (Katsuda et al., 2008). IXPE targeted the NW rim of Vela Jr (Prokhorov et al., 2024), which is the brightest in the X-rays, providing similar results to those obtained

for RX J1713, with a tangential magnetic field and a PD \sim 16% (right panel in Figure 4).

1.2 Diagnostic on turbulence through X-ray spectra

X-ray spectral analysis by itself is a powerful diagnostic tool to estimate the degree of turbulence in the plasma emitting X-ray synchrotron radiation, mainly through the estimate of the Bohm factor η . One of the most straightforward examples is provided by Tsuji et al. (2021), who systematically applied Equation 5 to a sample of SNRs characterized by nonthermal emission, to measure the value of η (see Figure 5).

They found that the Tycho's and Kepler's SNR nicely match the theoretical prediction, indicating a constant η across the various region considered. On the other hand, Cas A showed very different η values across regions with similar shock velocities. SN 1006 presented lower η values in correspondence of the nonthermal limbs, as expected given the configuration of the magnetic field and the efficiency of acceleration in the quasi-parallel scenario (Caprioli and Spitkovsky, 2014a). In their work, Tsuji et al. (2021) could not perform spatially resolved analysis for other SNRs and reported average values of $\eta \sim 1$ both for RX J1713 and Vela JR. Regarding Kepler's SNR, Sapienza et al. (2022) reported two different acceleration regimes between the north, site of interaction with a clump of CSM (Reynolds et al., 2007), and the south, where the shock wave is expanding freely. In the north they report values $\eta \sim 1$, while in the south $\eta \sim 6$.



Map of PD reported for the NE and SW limbs of SN 1006 from Zhou et al. (2023) and Zhou et al. (2025), in the left and right panels respectively. Vectors represent the direction of the magnetic field and their 1σ uncertainties, with blue corresponding to significance of $2-3\sigma$ and $>3\sigma$, respectively. White contours show the Stokes I levels.

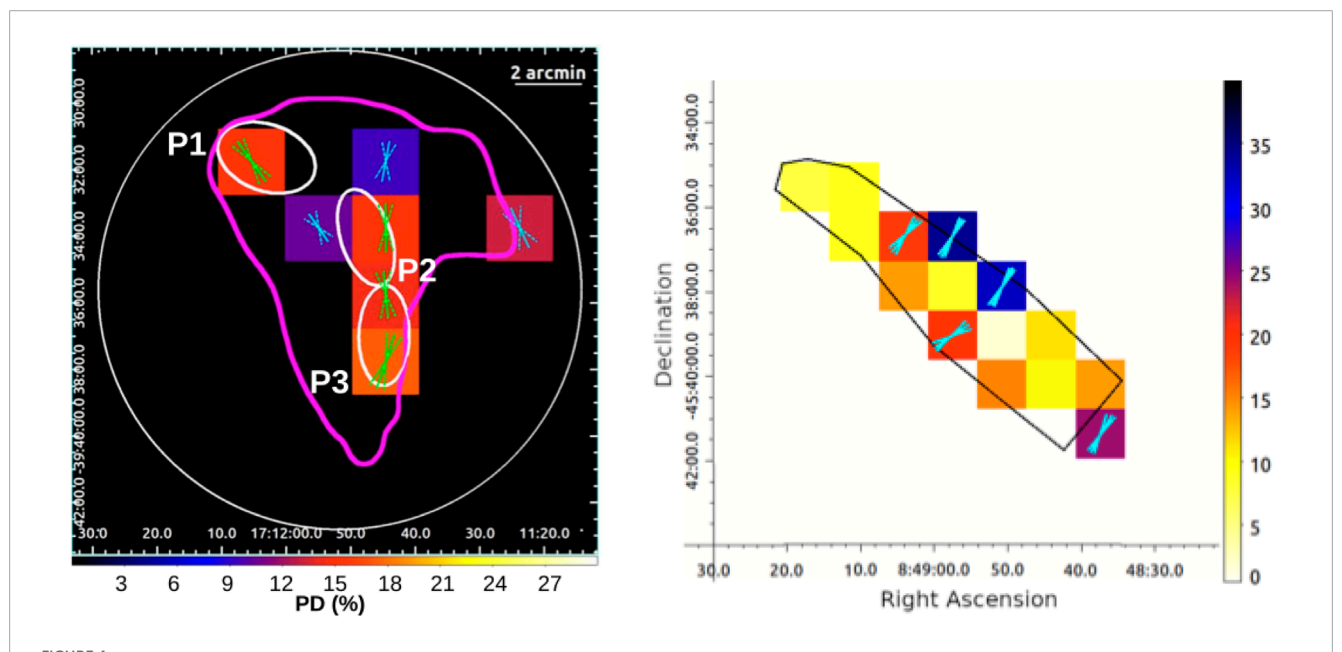
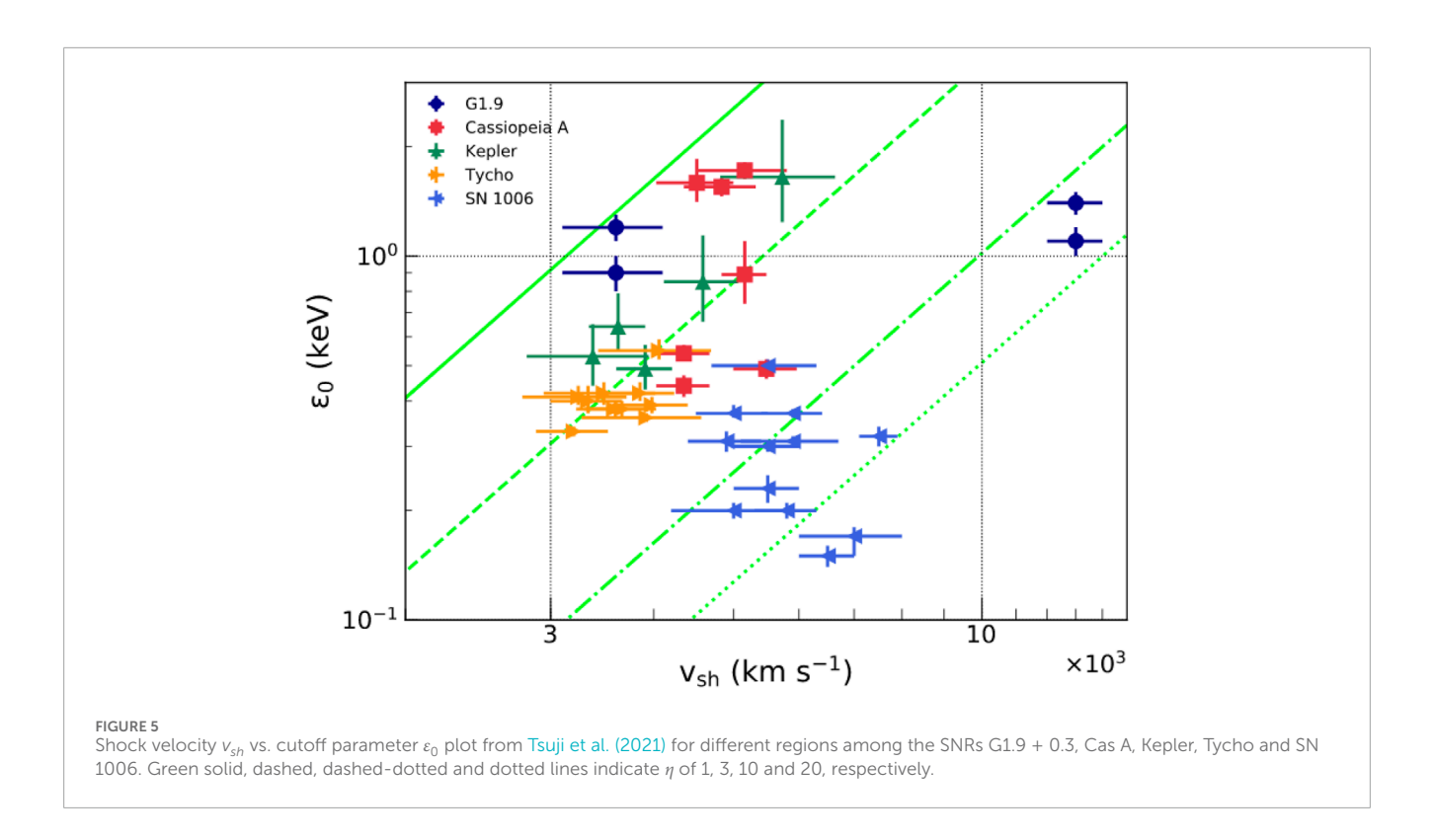


FIGURE 4 Left panel. PD and PA values reported for the NW area of RX J1713 from Ferrazzoli et al. (2024). Cyan and green vectors mark the magnetic field direction at the 2- and 3- σ significance level, respectively. Dashed vectors indicate the 2 σ uncertainty on the direction. The magenta line indicates the 2-5 keV IXPE contours. *Right panel*. Same as left panel but for the NW rim of Vela Jr from Prokhorov et al. (2024). The black line encloses all the pixels with significant X-ray flux.

Despite its crucial role in the DSA paradigm and the low PD observed, prevailing models used to fit X-ray nonthermal spectra of SNRs (e.g., SRcut by Reynolds and Keohane (1999), the loss-limited model by Zirakashvili and Aharonian (2007), or a

simple phenomenological power-law) are calculated assuming an homogeneous magnetic field. The resulting analytical expressions are typically power-law with a cutoff, with the shape of the cutoff depending mainly on whether the maximum energy of the electrons



is time-limited or loss-limited. Therefore, it is natural to ask what the emitted spectrum would look like by considering a turbulent magnetic field. This has been explored theoretically by Toptygin and Fleishman (1987) and Kelner et al. (2013), who labeled "jitter radiation" this emission process in which the electrons are sensitive also to the magnetic field's turbulent component. The resulting jitter radiation photon spectrum emitted from a power-law distribution of electrons can be described as a broken power-law having a smooth break between the regime dominated by standard synchrotron radiation (at lower energy) and that dominated by the jitter component (at higher energy). Interestingly, despite using different approximation and assumptions, both Toptygin and Fleishman (1987) and Kelner et al. (2013) agree on two striking features of jitter radiation: i) the slope of the spectrum at high energies is directly linked to the turbulence spectrum; ii) the maximum energy to which the spectrum extends is proportional to minimum scale of the turbulence. Jitter radiation is therefore a powerful tool that could provide direct diagnostics on turbulence parameters otherwise inaccessible for astrophysical sources. Greco et al. (2023) applied the jitter paradigm to the SNR Cas A, finding that it describes the X-ray broadband nonthermal spectra better than any standard cutoff model. They inferred an index in the turbulence spectrum v_B of 2–2.4, depending on the region considered, and an upper limit on the turbulence minimum scale of ~70 km. It is worth noting that in order for jitter radiation to be at work, the minimum scale of turbulence has also to be lower than the synchrotron formation length, since at larger scales the standard equations for synchrotron emission from electrons embedded in an homogeneous magnetic field would still be valid locally. Remarkably, for Cas A such criterion is satisfied, as the typical value for the synchrotron formation length is of $\sim 10^4$ km.

2 Discussion

In section 1 of this mini-review I briefly recalled the main recent results strictly related to the degree of turbulence and acceleration efficiency in the X-ray nonthermal emission of SNRs. The first clear takeaway is that acceleration efficiency - and, therefore, magnetic turbulence - is very high in most X-ray synchrotronemitting SNR, with the case of Vela Jr and RX J1713 showcasing the lowest values of Bohm factor η . I also showed that all the considered SNRs show PD much lower than the intrinsic limit, in line with the requirement of high magnetic turbulence for an highly efficient acceleration process. Some of these SNR present different acceleration regimes across different areas, depending on the conditions of the ambient environment and anisotropies. This is particularly true for Cas A and Kepler's SNR. The former is the SNR with the lowest X-ray polarization highlighting that it's evolving in a dense and inhomogeneous medium, relic of the progenitor star. Similarly, in the north the shock wave of Kepler's is interacting with a shell of CSM, and despite not being observed by IXPE yet, it shows an higher radio polarization in the south with respect to the north (DeLaney et al., 2002). On the other hand, SNRs such as SN 1006, RX J1713 and Vela Jr, which evolve in rarefied environment, show polarization levels higher than those observed in Cas A. These results indicate that while most of the turbulence responsible for the depolarization of the synchrotron radiation is intrinsically developed by the DSA mechanism, a secondary but definitely important role is also played by the preexisting medium. We are currently short of detailed simulations which investigate the acceleration process occurring in a shock expanding through a turbulent environment, and it is likely that combined effects of the instabilities intrinsically generated and the extrinsic

inhomogeneities in the ambient media could help us improve our understanding of the acceleration process and our interpretation of the PD values across different areas in SNRs.

It is important to notice that there is not necessarily a 1-to-1 relationship between the bohm factor η and the PD measured by IXPE. As also pointed out by Prokhorov et al. (2024), η quantifies the diffusion coefficient along the shock normal (Zirakashvili and Aharonian, 2007), while PD and PA depends on the distribution of the projected magnetic field onto the plane of the sky. This is a critical point for SNRs such as RX J1713 and Vela Jr, showing a tangential magnetic field, a relatively high polarization of 10% but a very efficient acceleration regime, having $\eta \approx 1$. The observed tangential polarization pattern indicates that only this component of the magnetic field retains a coherent structure, while the radial component is highly turbulent. Such radial disorder is exactly what one expects in a Bohm-like regime ($\eta \sim 1$), as reported for RX J1713 and Vela Jr and indicates a strongly anisotropic turbulence.

Turbulence does not always imply depolarization, especially in case in which there is a strong anisotropy, as has been shown for Tycho's SNR by Bykov et al. (2024). Anisotropic turbulence can also easily lead to ordered magnetic field structures that can increase the polarization level locally. For example, anisotropic turbulence may locally enhance/decrease the acceleration efficiency, inducing lower/higher values of η and of the radial polarization. This might be the case for some of the region in Cas A analysed by Vink et al. (2022) and Mercuri et al. (2025), who identified regions with PD levels even a factor ≈ six higher than the average on the whole shell. Naturally, it is not obvious to disentangle this kind of effects from the depolarization due to the mixing of the emission from different regions. The creation of coherent structures due to magnetic turbulence might sound counterintuitive, but it could explain, for example, also the flickering of X-ray hot spots reported by Uchiyama et al. (2007) for RX J1713: fluctuations might generate extremely high (~mG) magnetic field in localized regions. One would expect that radiation stemming from these spots is highly unpolarized, but this may not be entirely true because of, again, the putative different orientation on the magnetic field with respect to the shock normal. IXPE has not the capability to resolve arcsecond-like structures, but an hint on this could be achieved by cross relating the regions characterized by lower magnetic field (i.e., less amplified and therefore less turbulent) with those having higher PD values. Remembering that magnetic field is better amplified in faster shocks, the velocity of the shock could be used as first key parameter to identify the most promising regions, excluding cases with clear interaction with significantly denser media.

In Sect. 1 I also described a new potential spectroscopic diagnostic tool on turbulence, based on the jitter radiation paradigm. The only application on SNR was performed by Greco et al. (2023) on Cas A. They found a turbulence spectrum steeper than the typical Kolmogorov value of $v_B = 5/3$, suggesting that different form of instabilities might be at work. Surprisingly, the turbulence scales inferred are much lower than those considered for magnetic turbulence responsible for acceleration, of the order of ~100 km. This point is not necessarily an issue since in the jitter framework the inclusion of a turbulent component in the magnetic field only affects the emission of photons

and not the acceleration process. It might be more questionable, and future studies are needed in this sense, whether turbulence can actually survive at this scale. w In general, the jitter radiation process needs to be tested and validated in a more systematic way for several other SNRs. In this framework, a decisive signature would be a systematic correlation between the PD measured by IXPE and the jitter break energy: a higher break energy would indicate that the intrinsically polarized synchrotron component dominates in the 4–6 keV band, whereas a lower break energy would imply that the intrinsically unpolarized jitter component already prevails in this range.

3 Conclusion

In this mini-review I summarized some of the most relevant recent results inferred from X-ray polarimetric and spectral analysis relative to magnetic turbulence in SNRs. The current picture clearly shows that turbulence is a key ingredient in the acceleration and X-ray emission mechanism in SNRs. Thanks to the IXPE telescope it is now possible to measure the PD and PA in several SNRs. These unprecedented information coupled with the results obtained on the curvature of the X-ray nonthermal spectra show that every synchrotron-emitting SNR is characterized by turbulence, mainly self-generated by the expanding shock. However, also the configuration of the pre-existing medium seems to play a significant role. Additional observations and numerical simulations are needed to better understand to what extent the preexisting medium affects the acceleration and emission processes.

Author contributions

EG: Writing – original draft, Writing – review and editing.

Funding

The author(s) declare that financial support was received for the research and/or publication of this article. E.G., acknowledge support from the INAF Minigrant RSN4 "Investigating magnetic turbulence in young Supernova Remnants through X-ray observations".

Acknowledgements

E.G., acknowledge discussion and collaboration with colleagues M. Miceli, S. Orlando, J. Vink, A. Mercuri, S. Perri, D. Caprioli.

Conflict of interest

The author declares that the research was conducted in the absence of any commercial or financial relationships that could be construed as a potential conflict of interest.

Generative AI statement

The author(s) declare that no Generative AI was used in the creation of this manuscript.

Any alternative text (alt text) provided alongside figures in this article has been generated by Frontiers with the support of artificial intelligence and reasonable efforts have been made to ensure accuracy, including review by the authors wherever possible. If you identify any issues, please contact us.

References

Anderson, M. C., Keohane, J. W., and Rudnick, L. (1995). The polarization and depolarization of radio emission from supernova remnant cassiopeia A. *ApJ* 441, 300. doi:10.1086/175356

Bell, A. R. (2004). Turbulent amplification of magnetic field and diffusive shock acceleration of cosmic rays. *MNRAS* 353, 550–558. doi:10.1111/j.1365-2966.2004.08097.x

Blandford, R., and Eichler, D. (1987). Particle acceleration at astrophysical shocks - a theory of cosmic-ray origin. PhR 154, 1–+75. doi:10.1016/0370-1573(87)90134-7

Blasi, P. (2013). The origin of galactic cosmic rays. A&AR 21, 70. doi:10.1007/s00159-013-0070-7

Bykov, A. M., Uvarov, Y. A., Slane, P., and Ellison, D. C. (2020). Uncovering magnetic turbulence in young supernova remnants with polarized X-Ray imaging. *ApJ* 899, 142. doi:10.3847/1538-4357/aba960

Bykov, A. M., Osipov, S. M., Uvarov, Y. A., Ellison, D. C., and Slane, P. (2024). X-ray polarization: a view deep inside cosmic ray driven turbulence and particle acceleration in supernova remnants. *PhysRevD* 110, 023041. doi:10.1103/PhysRevD.110.023041

Caprioli, D., and Spitkovsky, A. (2014a). Simulations of ion acceleration at non-relativistic shocks. I. Acceleration efficiency. *ApJ* 783, 91. doi:10.1088/0004-637X/783/2/91

Caprioli, D., and Spitkovsky, A. (2014b). Simulations of ion acceleration at non-relativistic shocks. II. Magnetic field amplification. *ApJ* 794, 46. doi:10.1088/0004-637X/794/1/46

DeLaney, T., Koralesky, B., Rudnick, L., and Dickel, J. R. (2002). Radio spectral index variations and physical conditions in Kepler's Supernova remnant. $ApJ\ 580,\ 914-927.$ doi:10.1086/343787

Dickel, J. R., van Breugel, W. J. M., and Strom, R. G. (1991). Radio structure of the remnant of tycho's Supernova (SN 1572). AJ 101, 2151. doi:10.1086/115837

Eriksen, K. A., Hughes, J. P., Badenes, C., Fesen, R., Ghavamian, P., Moffett, D., et al. (2011). Evidence for particle acceleration to the knee of the cosmic ray spectrum in Tycho's Supernova remnant. *ApJL* 728, L28. doi:10.1088/2041-8205/728/J178

Fermi, E. (1949). On the origin of the cosmic radiation. *Phys. Rev.* 75, 1169-1174. doi:10.1103/PhysRev.75.1169

Ferrazzoli, R., Slane, P., Prokhorov, D., Zhou, P., Vink, J., Bucciantini, N., et al. (2023). X-Ray polarimetry reveals the magnetic-field topology on sub-parsec scales in Tycho's Supernova remnant. *ApJ* 945, 52. doi:10.3847/1538-4357/acb496

Ferrazzoli, R., Prokhorov, D., Bucciantini, N., Slane, P., Vink, J., Cardillo, M., et al. (2024). Discovery of a shock-compressed magnetic field in the Northwestern rim of the young Supernova remnant RX J1713.7–3946 with X-Ray polarimetry. *ApJL* 967, L38. doi:10.3847/2041-8213/ad4a68

Ginzburg, V. L., and Syrovatskii, S. I. (1965). Cosmic Magnetobremsstrahlung (synchrotron Radiation). ARA &A 3, 297–350 doi:10.1146/annurev.aa.03.090165.001501

Greco, E., Vink, J., Ellien, A., and Ferrigno, C. (2023). Jitter radiation as an alternative mechanism for the Nonthermal X-Ray emission of cassiopeia A. *ApJ* 956, 116. doi:10.3847/1538-4357/acf567

Helder, E. A., Vink, J., Bykov, A. M., Ohira, Y., Raymond, J. C., and Terrier, R. (2012). Observational signatures of particle acceleration in Supernova remnants. *SSR* 173, 369–431. doi:10.1007/s11214-012-9919-8

Inoue, T., Shimoda, J., Ohira, Y., and Yamazaki, R. (2013). The origin of radially aligned magnetic fields in young Supernova remnants. *ApJL* 772, L20. doi:10.1088/2041-8205/772/2/L20

Katsuda, S., Tsunemi, H., and Mori, K. (2008). The slow X-Ray expansion of the Northwestern rim of the Supernova remnant RX J0852.0-4622. *ApJL* 678, L35–L38. doi:10.1086/588499

Publisher's note

All claims expressed in this article are solely those of the authors and do not necessarily represent those of their affiliated organizations, or those of the publisher, the editors and the reviewers. Any product that may be evaluated in this article, or claim that may be made by its manufacturer, is not guaranteed or endorsed by the publisher.

Katsuda, S., Acero, F., Tominaga, N., Fukui, Y., Hiraga, J. S., Koyama, K., et al. (2015). Evidence for thermal X-Ray line emission from the synchrotron-dominated Supernova remnant RX J1713.7-3946. *ApJ* 814, 29. doi:10.1088/0004-637X/814/1/29

Kelner, S. R., Aharonian, F. A., and Khangulyan, D. (2013). On the jitter radiation. ApJ 774, 61. doi:10.1088/0004-637X/774/1/61

Kothes, R., Sun, X., Gaensler, B., and Reich, W. (2018). A radio continuum and polarization Study of SNR G57.2+0.8 associated with magnetar SGR 1935+2154. *ApJ* 852, 54. doi:10.3847/1538-4357/aa9e89

Koyama, K., Petre, R., Gotthelf, E. V., Hwang, U., Matsura, M., Ozaki, M., et al. (1995). Evidence for shock acceleration of high-energy electrons in the supernova remnant sn:1006. *Nature* 378, 255–258. doi:10.1038/378255a0

Malkov, M. A., and O'C Drury, L. (2001). Nonlinear theory of diffusive acceleration of particles by shock waves. $Rep.\ Prog.\ Phys.\ 64,429-481.\ doi:10.1088/0034-4885/64/4/201$

Matsuda, M., Tanaka, T., Uchida, H., Amano, Y., and Tsuru, T. G. (2020). Temporal and spatial variation of synchrotron X-ray stripes in Tycho's supernova remnant. *PASJ* 72, 85. doi:10.1093/pasj/psaa075

Mercuri, A., Greco, E., Vink, J., Ferrazzoli, R., and Perri, S. (2025). Revisiting the X-Ray polarization of the shell of cassiopeia A using spectropolarimetric analysis. *ApJ* 986, 6. doi:10.3847/1538-4357/adcedb

Meshkov, E. E. (1969). Instability of the interface of two gases accelerated by a shock wave. Fluid Dyn. 4, 101–104. doi:10.1007/BF01015969

Miceli, M., Acero, F., Dubner, G., Decourchelle, A., Orlando, S., and Bocchino, F. (2014). Shock-Cloud interaction and particle acceleration in the Southwestern limb of SN 1006. *ApJL* 782, L33. doi:10.1088/2041-8205/782/2/L33

Parizot, E., Marcowith, A., Ballet, J., and Gallant, Y. A. (2006). Observational constraints on energetic particle diffusion in young supernovae remnants: amplified magnetic field and maximum energy. *A&A* 453, 387–395. doi:10.1051/0004-6361:20064985

Prokhorov, D. A., Yang, Y.-J., Ferrazzoli, R., Vink, J., Slane, P., Costa, E., et al. (2024). Evidence for a shock-compressed magnetic field in the northwestern rim of vela jr. from X-ray polarimetry. *A&A* 692, A59. doi:10.1051/0004-6361/202452062

Reynolds, S. P., and Keohane, J. W. (1999). Maximum energies of shock-accelerated electrons in young shell supernova remnants. *ApJ* 525, 368–374. doi:10.1086/

Reynolds, S. P., Borkowski, K. J., Hwang, U., Hughes, J. P., Badenes, C., Laming, J. M., et al. (2007). A deep chandra observation of Kepler's Supernova remnant: a type Ia event with circumstellar interaction. *ApJL* 668, L135–L138. doi:10.1086/522830

Reynoso, E. M., Hughes, J. P., and Moffett, D. A. (2013). On the radio polarization signature of efficient and inefficient particle acceleration in Supernova remnant SN 1006. AJ 145, 104. doi:10.1088/0004-6256/145/4/104

Richmyer, R. D. (1960). Taylor instability in shock acceleration of compressible fluids. *Commun. Pure Appl. Math.* XIII, 297–319. doi:10.1002/cpa.3160130207

Rosenberg, I. (1970). Distribution of brightness and polarization in Cassiopeia A at 5.0 GHz. MNRAS 151, 109–122. doi:10.1093/mnras/151.1.109

Sapienza, V., Miceli, M., Bamba, A., Katsuda, S., Nagayoshi, T., Terada, Y., et al. (2022). A spatially resolved Study of hard X-Ray emission in Kepler's Supernova remnant: indications of different regimes of particle acceleration. *ApJ* 935, 152. doi:10.3847/1538-4357/ac8160

Sapienza, V., Miceli, M., Petruk, O., Bamba, A., Katsuda, S., Orlando, S., et al. (2024). Time evolution of the synchrotron X-Ray emission in Kepler's Supernova remnant: the effects of turbulence and shock velocity. *ApJ* 973, 105. doi:10.3847/1538-4357/ad6566

Toptygin, I. N., and Fleishman, G. D. (1987). A role of cosmic-rays in generation of radio and optical radiation by plasma mechanisms. *Ap&SS* 132, 213–248. doi:10.1007/BF00641755

Tsuji, N., Uchiyama, Y., Khangulyan, D., and Aharonian, F. (2021). Systematic Study of acceleration efficiency in young Supernova remnants with nonthermal X-Ray observations. *ApJ* 907, 117. doi:10.3847/1538-4357/abce65

Uchiyama, Y., Aharonian, F. A., Tanaka, T., Takahashi, T., and Maeda, Y. (2007). Extremely fast acceleration of cosmic rays in a supernova remnant. *Nature* 449, 576–578. doi:10.1038/nature06210

- Vink, J. (2006). "X-ray high resolution and imaging spectroscopy of Supernova remnants". *Proceedings of the X-ray Universe* 2005 (Esa Special Publication), 319.
- Vink, J. (2020). Physics and evolution of Supernova remnants. Springer. $\mbox{doi:}10.1007/978\text{-}3\text{-}030\text{-}55231\text{-}2$
- Vink, J., and Laming, J. M. (2003). On the magnetic fields and particle acceleration in cassiopeia A. ApJ~584,~758-769. doi:10.1086/345832
- Vink, J., Prokhorov, D., Ferrazzoli, R., Slane, P., Zhou, P., Asakura, K., et al. (2022). X-ray polarization detection of cassiopeia A with IXPE. *arXiv e-prints* 938, 40. doi:10.3847/1538-4357/ac8b7b
- Weisskopf, M. C., Soffitta, P., Baldini, L., Ramsey, B. D., O'Dell, S. L., Romani, R. W., et al. (2022). Imaging X-ray polarimetry explorer: prelaunch. *J. Astronomical Telesc. Instrum. Syst.* 8, 026002. doi:10.1117/1.JATIS.8.2.026002

- Williams, B. J., Chomiuk, L., Hewitt, J. W., Blondin, J. M., Borkowski, K. J., Ghavamian, P., et al. (2016). An X-Ray and radio Study of the varying expansion velocities in Tycho's Supernova remnant. *ApJL* 823, L32. doi:10.3847/2041-8205/823/2/L32
- Xu, J. W., Han, J. L., Sun, X. H., Reich, W., Xiao, L., Reich, P., et al. (2007). Polarization observations of SNR G156.2+5.7 at λ6 Cm. A&A 470, 969–975. doi:10.1051/0004-6361:20077549
- Zhou, P., Prokhorov, D., Ferrazzoli, R., Yang, Y.-J., Slane, P., Vink, J., et al. (2023). Magnetic structures and turbulence in SN 1006 revealed with imaging X-Ray polarimetry. *ApJ* 957, 55. doi:10.3847/1538-4357/
- Zhou, P., Slane, P., Prokhorov, D., Vink, J., Ferrazzoli, R., Cotton, W., et al. (2025). X-Ray polarization in SN 1006 Southwest shows spatial variations and differences in the radio band. *ApJ* 986, 210. doi:10.3847/1538-4357/add532
- Zirakashvili, V. N., and Aharonian, F. (2007). Analytical solutions for energy spectra of electrons accelerated by nonrelativistic shock-waves in shell type supernova remnants. A&A 465, 695–702. doi:10.1051/0004-6361: 20066494